

OVATION Prime: A New Generation Auroral Precipitation Model with Comparative Testing

T. Sotirelis, P. T. Newell and S. Wing

The Johns Hopkins University

Applied Physics Laboratory

Laurel, Maryland, 20723

Space Weather Applications of Auroral Precipitation Forecast/Nowcast?

- Provide location of ionospheric irregularities caused by auroral precipitation which interfere with communications/radar/GPS
- Provide accurate input to Ionosphere–Thermosphere (IT) predictive models, which propagate auroral impacts worldwide.
- Understand satellite anomalies caused by surface charging

Why Do We Need Another Precipitation Model?

- There are actually four different types of aurora
- Each type has a different dependence on IMF/substorm cycle/Kp
- There are strong seasonal effects which are different for each kind of aurora
- The aurora does not jump between a handful of fixed levels

Types of Auroral Precipitation

Discrete (*electron acceleration*)

--Monoenergetic: Most of the energy flux is in one or two DMSP channels.

Source: quasi-static electric fields

--Broadband: Electron acceleration over three or more DMSP channels.

Source: Dispersive Alfvén waves (DAWs).

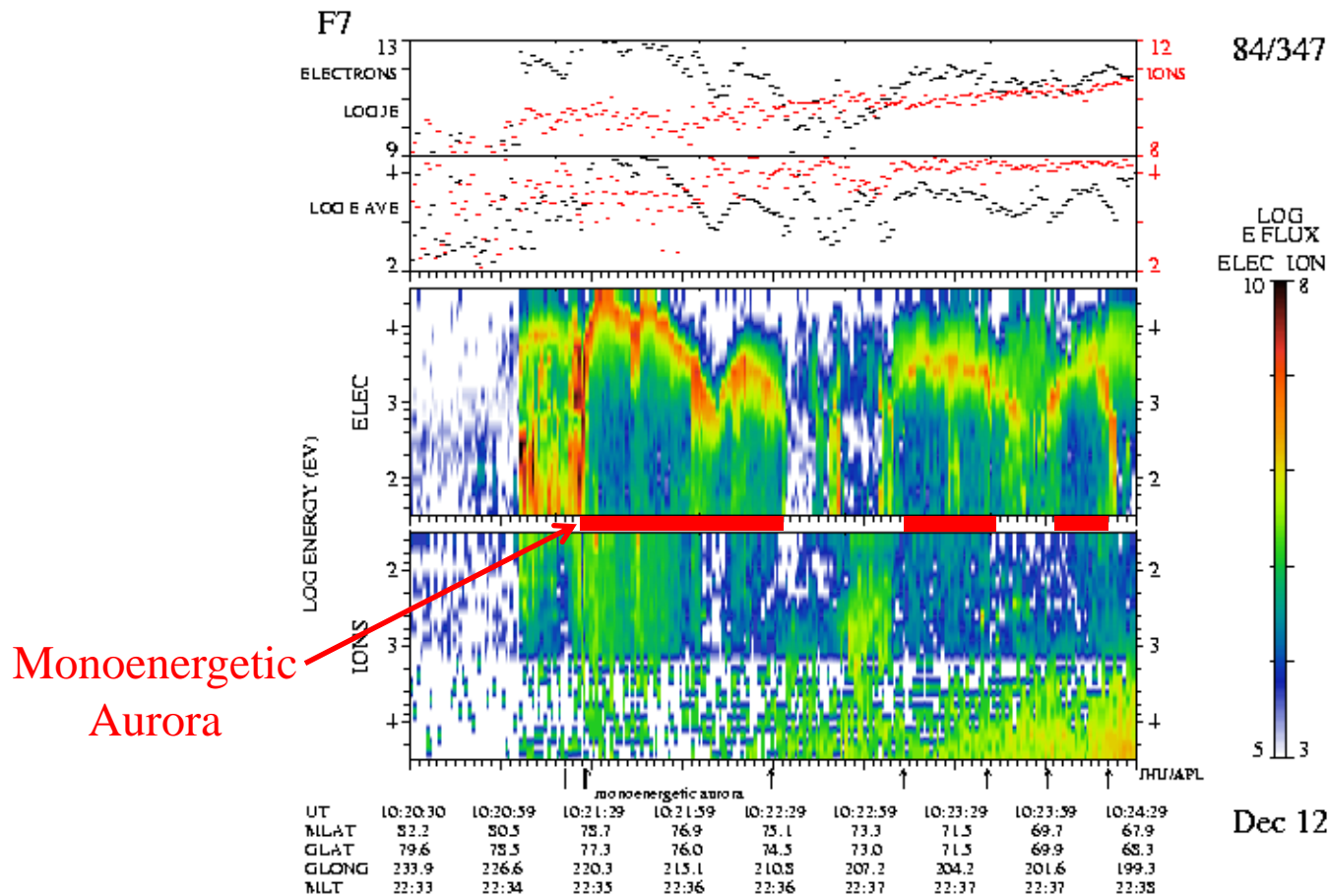
Diffuse (*unaccelerated*)

--Electron

--Ion

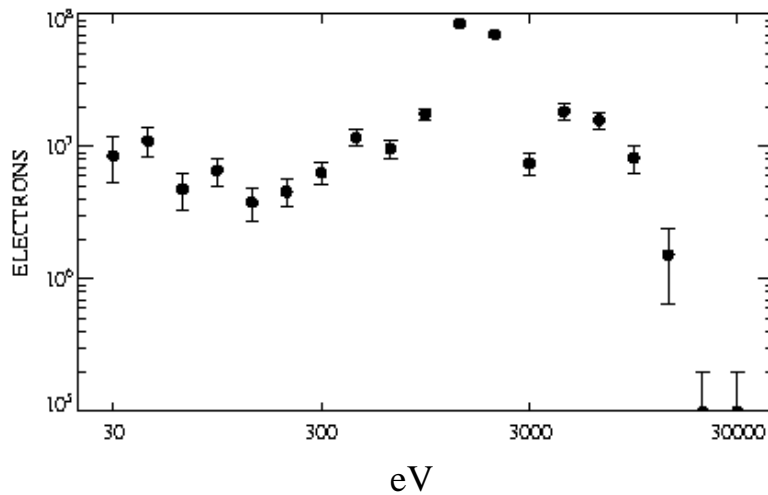
Most of the energy flux is e^- , because the light e^- mass (and thus high v) outweighs the higher ion energy density.

Example Of Monoenergetic Aurora

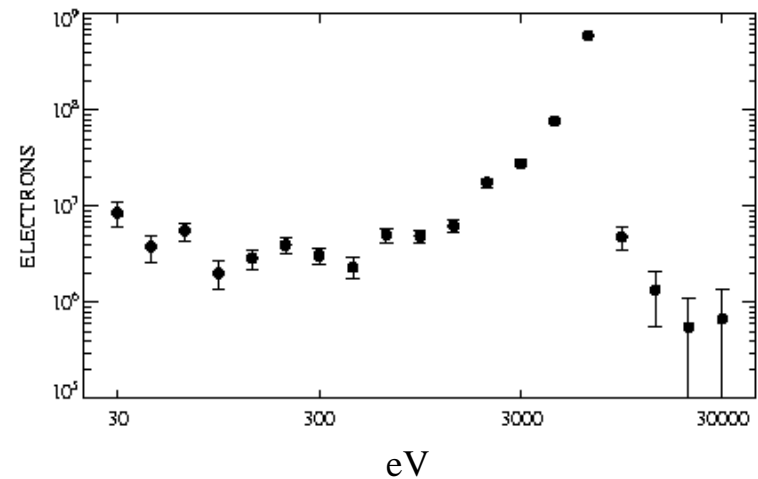


Examples of Monoenergetic Peaks

DMSP F13 1996/166 02:07:44

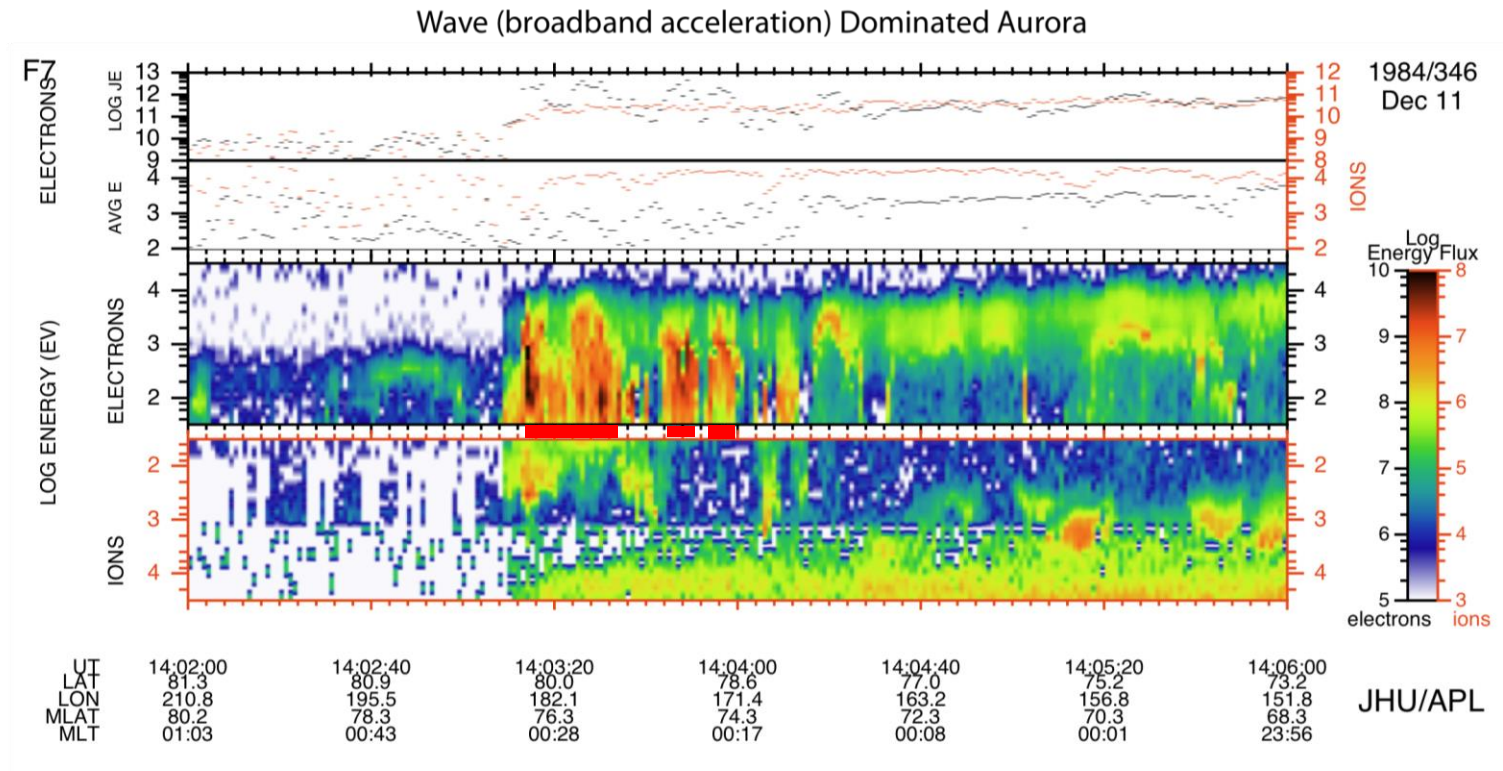


DMSP F12 1996/169 01:31:24



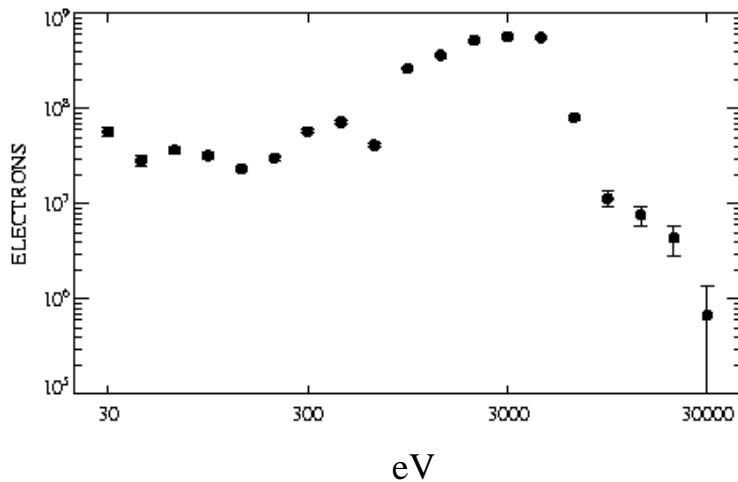
Differential Directional Energy Flux in $\text{eV}/(\text{eV cm}^2 \text{ sec. sr.})$

Example of Broadband Dominated Aurora

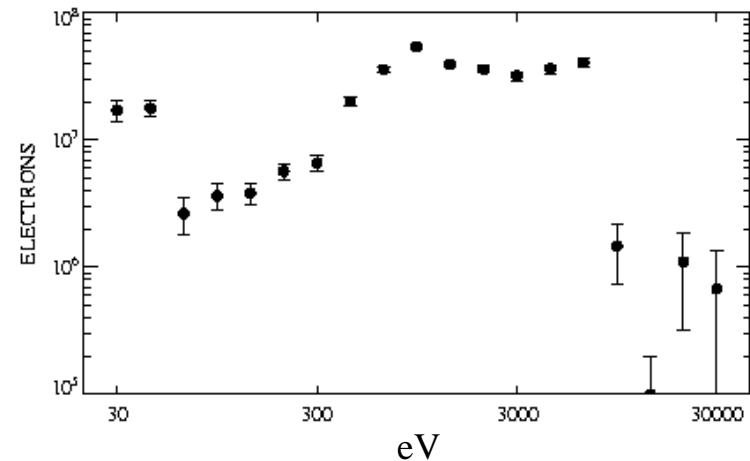


Examples of Broadband Accelerated Electron Spectra

DMSP F12 1996/170 23:24:54

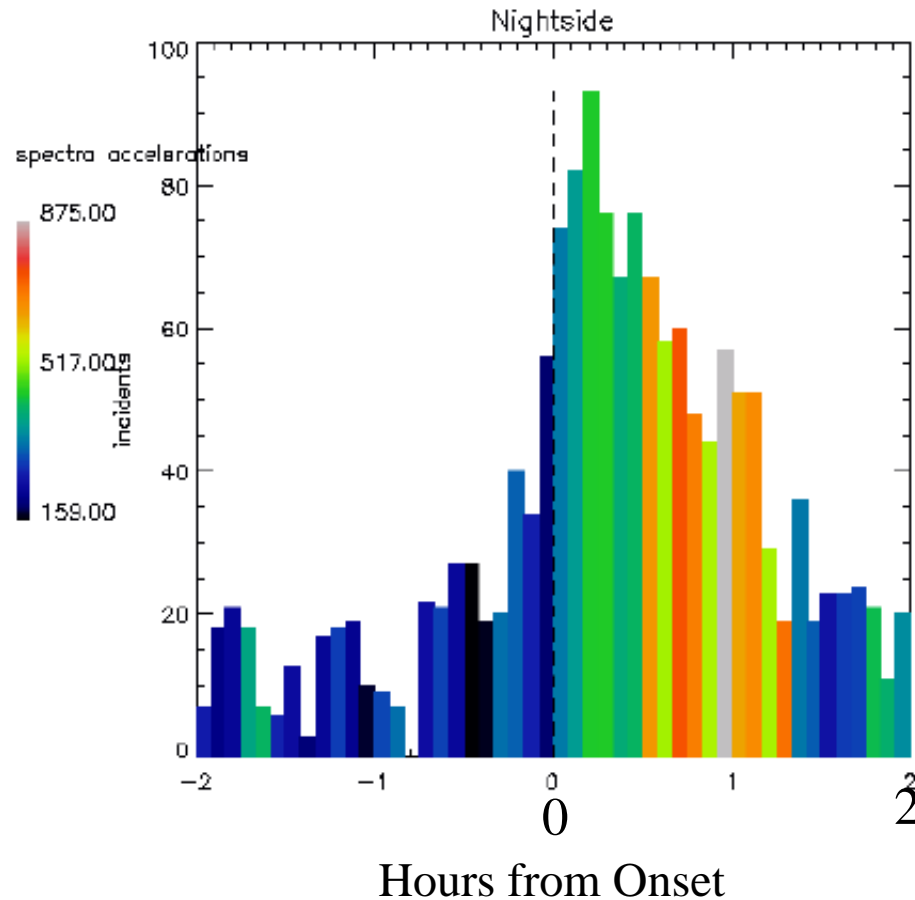


DMSP F12 1996/170 23:24:51



Differential Directional Energy Flux in $\text{eV}/(\text{eV cm}^2 \text{ sec. sr.})$

Low-latitude Wave Aurora Near Substorm Onset: Superposed Epoch Analysis



A. R. Lee, P. T. Newell, J. Gjerloev, and K. Liou (2010), Relatively low-latitude wave aurora and substorms, *Geophys. Res. Lett.*, 37, L06101, doi:10.1029/2009GL041680.

Criteria for Sorting Auroral Types

- *Accelerated* (or “discrete”) if 1 or more channel has $dj_E/dE > 10^8 \text{ eV/cm}^2 \text{ s sr eV}$ (necessary but not sufficient condition)
- *Monoenergetic* (quasi-static electric fields) if only 1 or 2 channels dominate (factor of 5 > other channels)
- *Broadband* (“wave”) if 3 or more channels are $> 2 \times 10^8 \text{ eV/cm}^2 \text{ s sr eV}$

Model Parameterization

- Functional fit versus solar wind (rather than bins)
- Each type of aurora fitted separately
- Each MLT/MLAT bin fitted separately
- Solar wind driving based on

$$d\Phi_{\text{MP}}/dt = v_{\text{SW}}^{4/3} B_T^{2/3} \sin^{8/3}(\theta_C/2)$$

“Low” (or quiet) here is $0.25 \langle d\Phi_{\text{MP}}/dt \rangle$

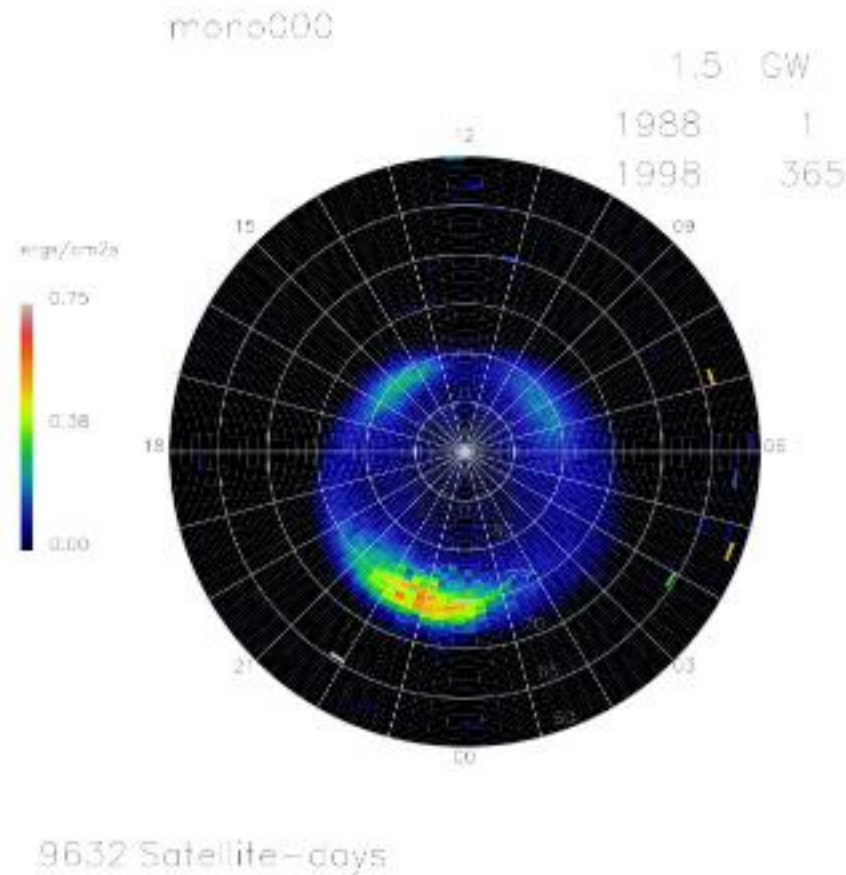
“High” (or active) here is $1.5 \langle d\Phi_{\text{MP}}/dt \rangle$

Model Construction

- 4 auroral types x 96 MLT bins x 120 MLAT bins = 46,080 regression equations
- Auroral power(mlat_bin, mlt_bin, aurora_type) = $a + b \cdot d\Phi_{MP}/dt$
- The same is done for number flux (46,080 more regressions)
- The probability of observing each type of electron aurora is also fit with a similar regression equation.
- There is only one type of ion aurora, so there is no probability fit
- Total flux is the product of the probability of observing an aurora times the flux when present.
- This can be evaluated for any solar wind history (the IMF for the last 3 hours is used here)

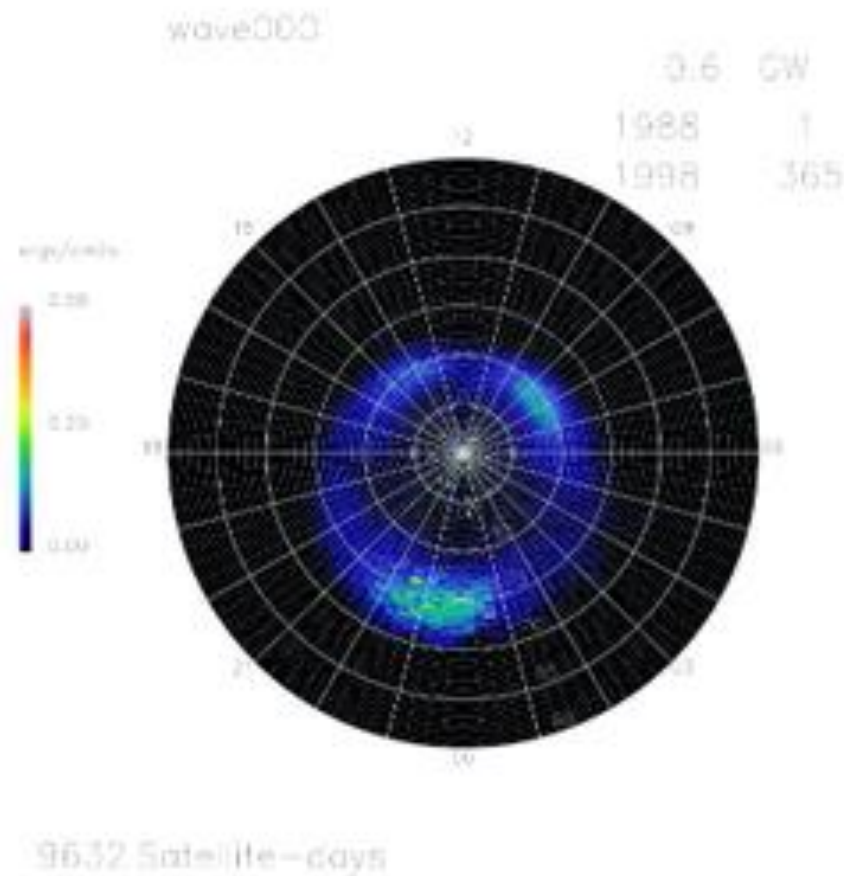
Monoenergetic Aurora Energy Flux

1.5-10 GW



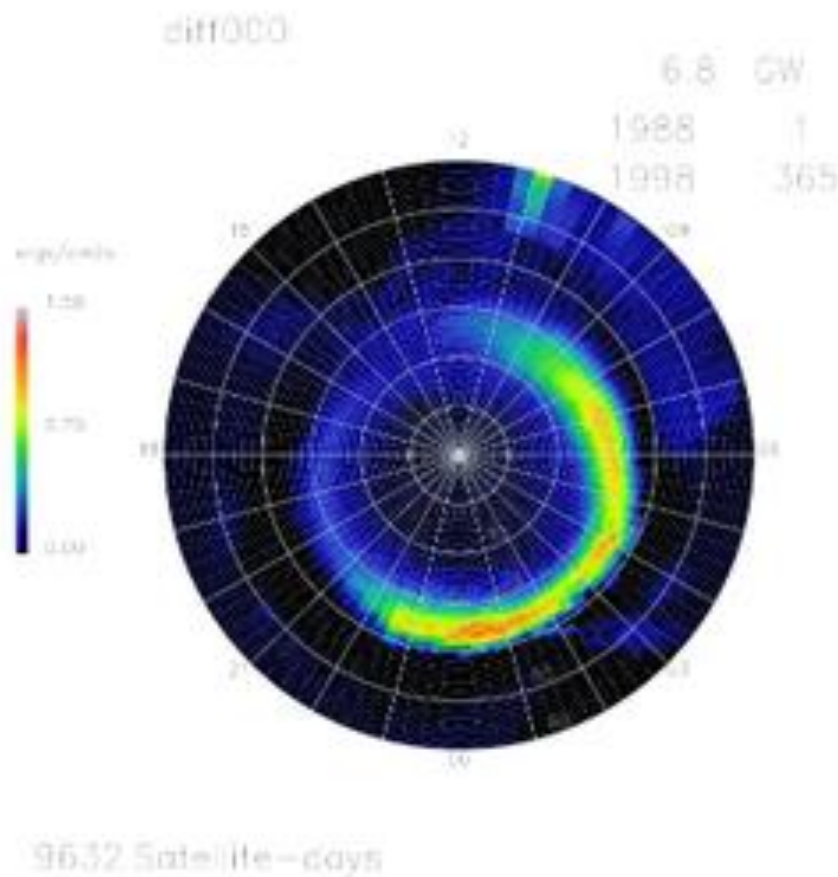
Broadband (Wave) Aurora Energy Flux

0.6-6 GW



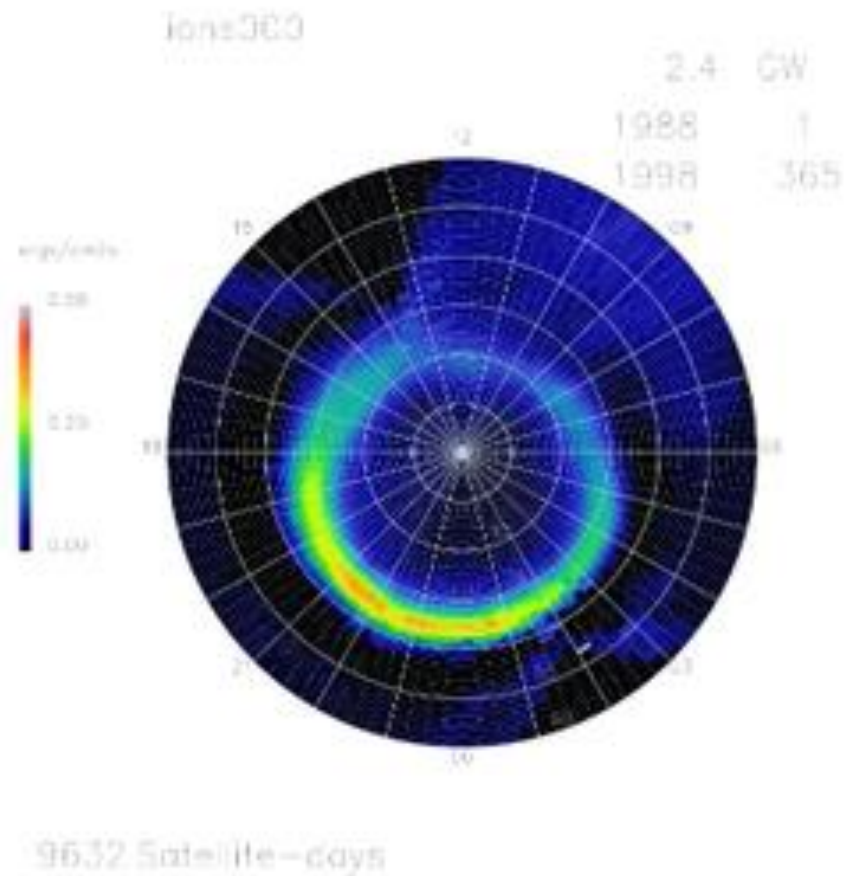
Diffuse e^- Aurora Energy Flux

7-25 GW

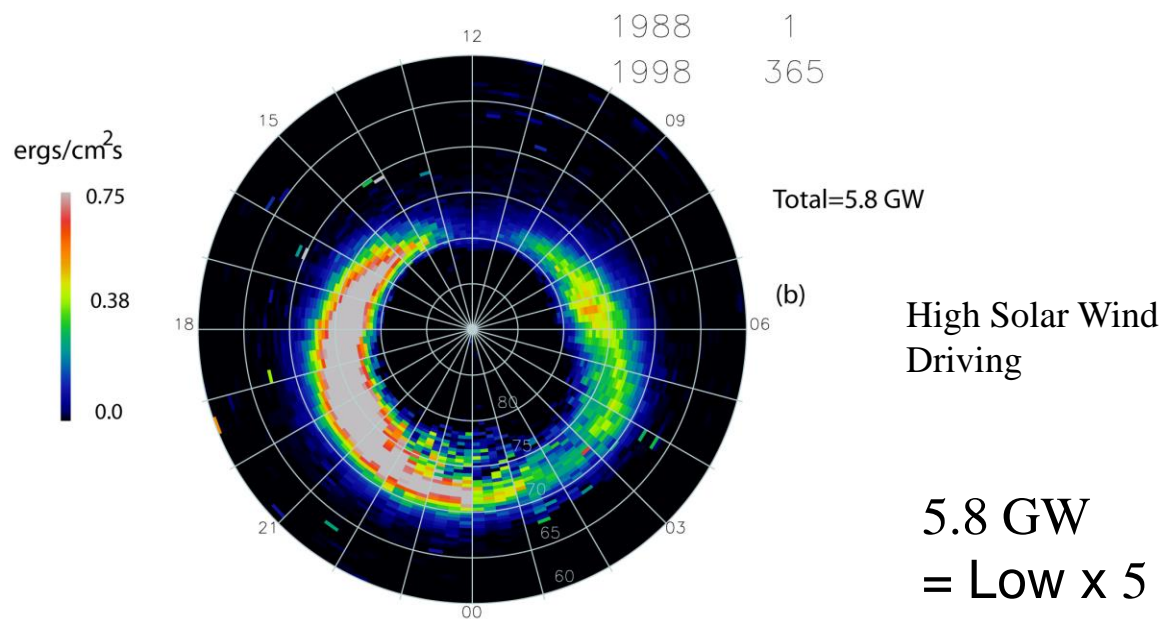
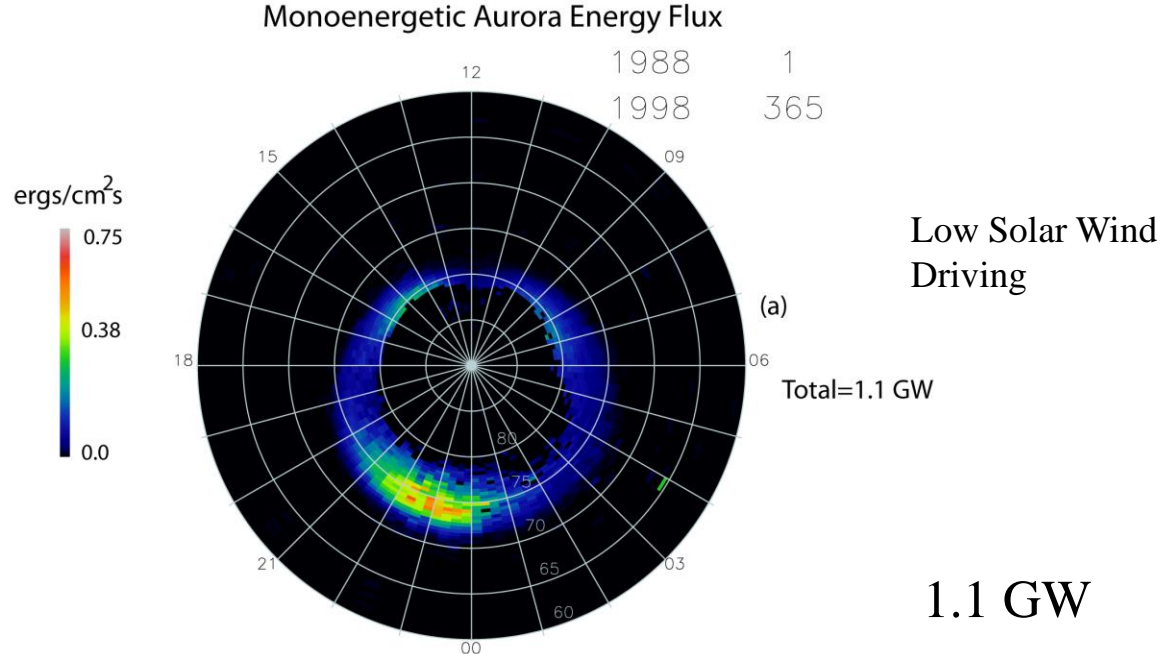


Ion Aurora Energy Flux

2.4-6 GW

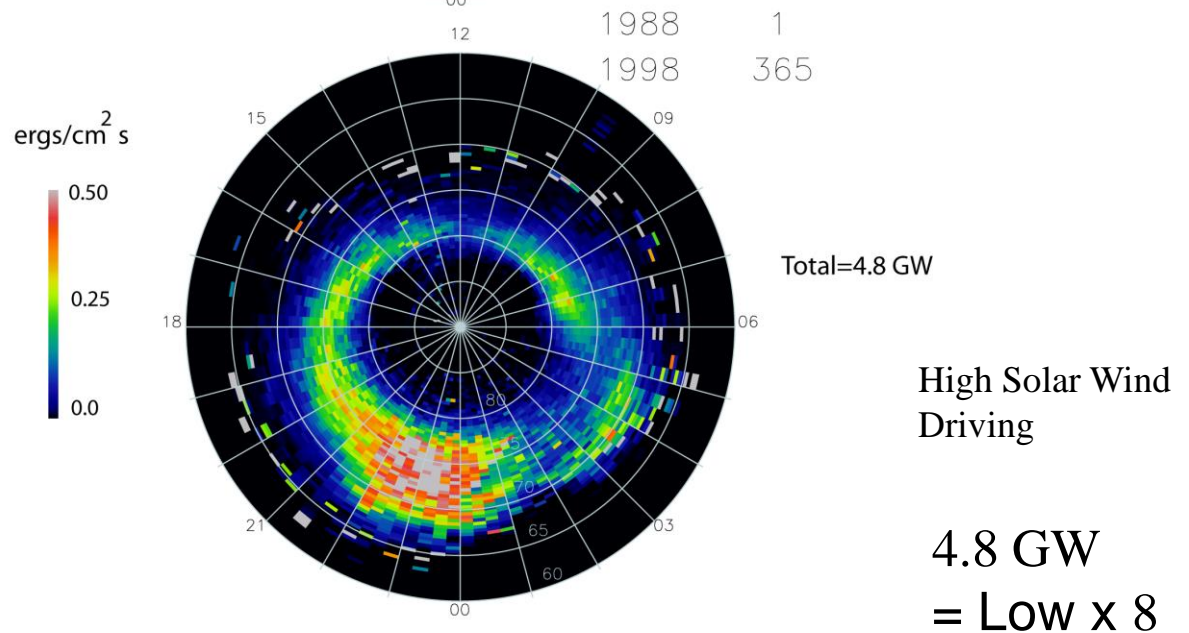
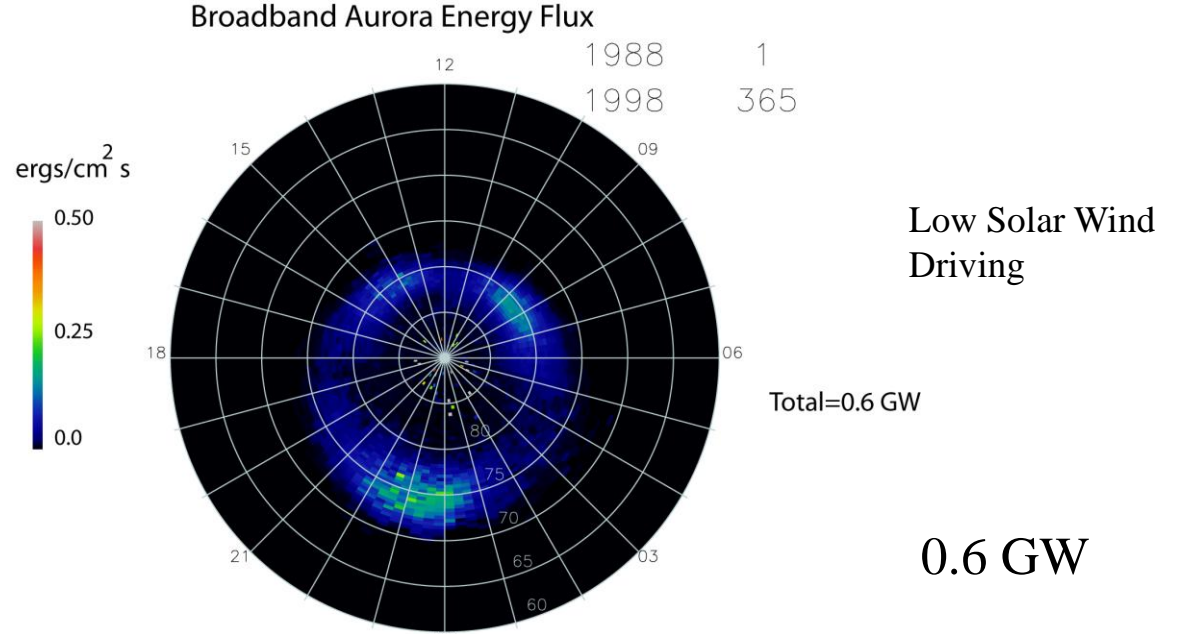


Monoenergetic Aurora Energy Flux



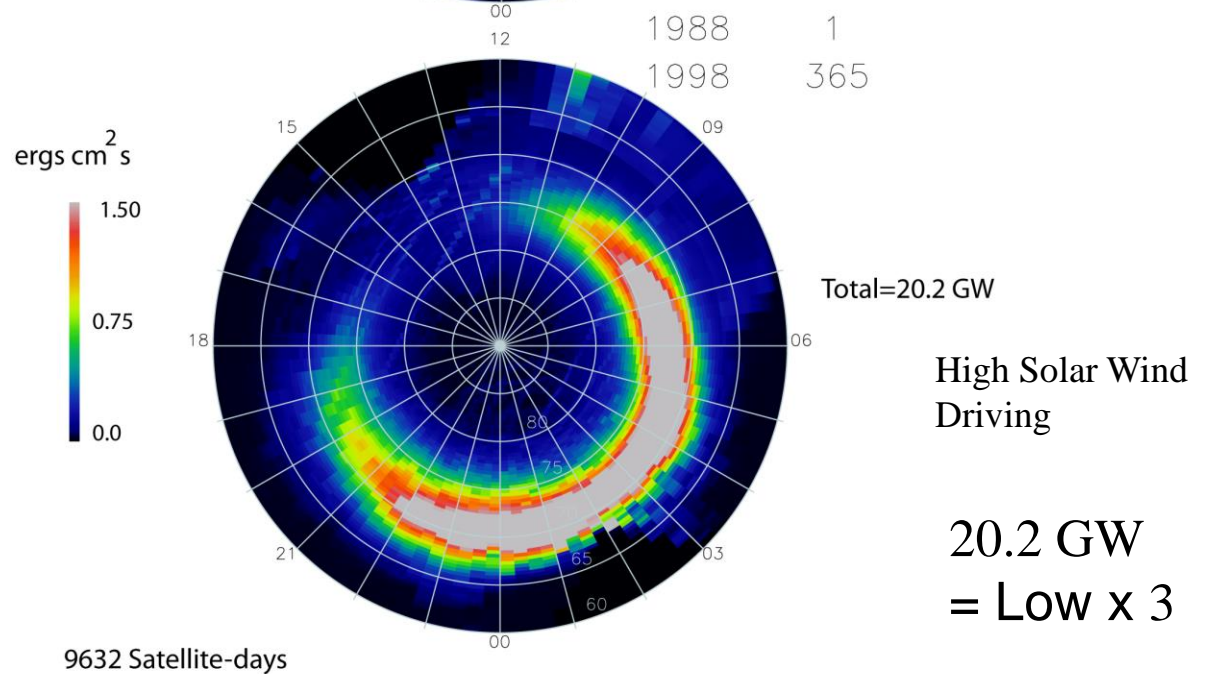
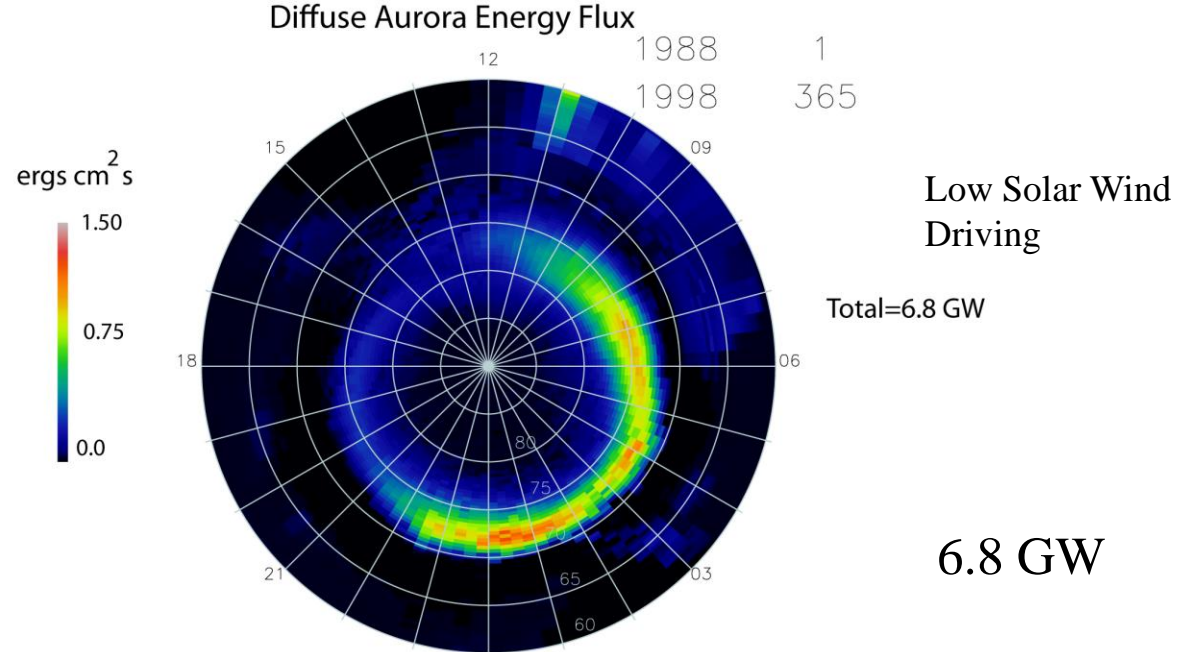
9632 Satellite-days

Broadband (Wave) Aurora Energy Flux

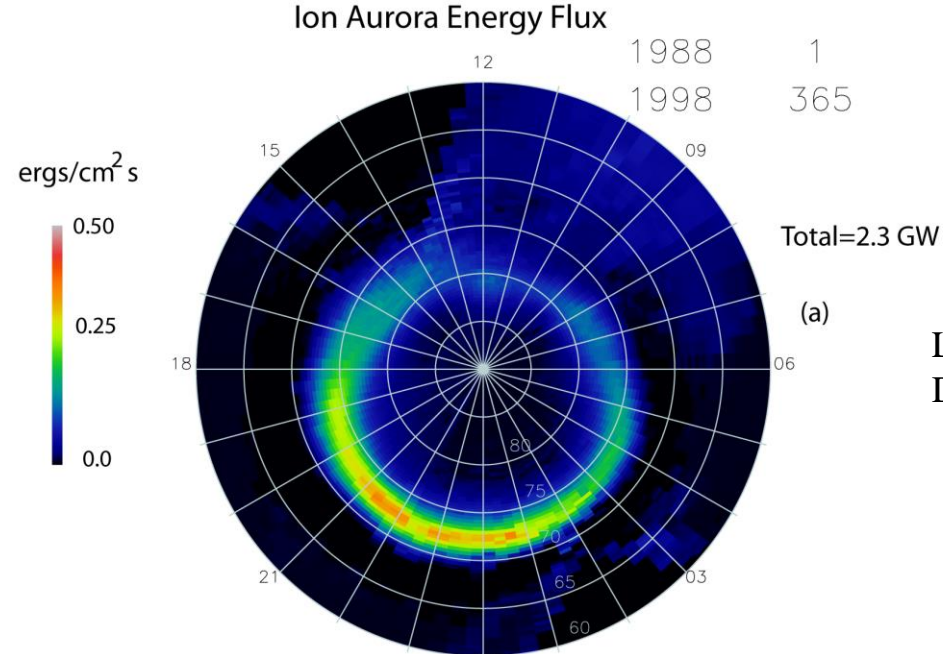


9632 Satellite-days

Diffuse e⁻ Aurora Energy Flux

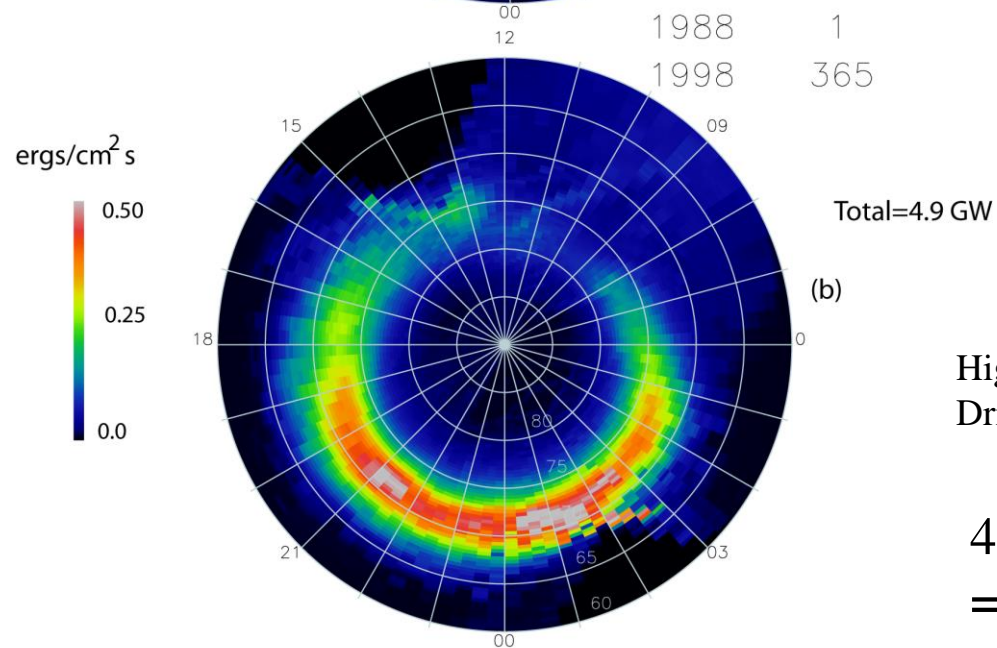


Ion Aurora Energy Flux



Low Solar Wind
Driving

2.3 GW



High Solar Wind
Driving

4.9 GW
= Low x 2

9632 Satellite-days

Relative Contributions to Hemispheric Precipitating Energy Flux

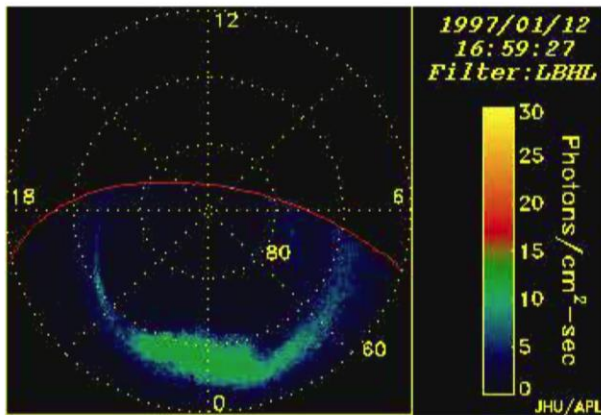
Aurora Type	Hemispheric Power: Quiet (Gigawatts)	Hemispheric Power: Active (Gigawatts)	Hemispheric Power: All Conditions Gigawatts
Diffuse (e-)	6.8 (63%)	20.2 (57%)	12.6 (61%)
Diffuse (ion)	2.3 (21%)	4.9 (14%)	3.4 (16%)
Monoenergetic	1.1 (10%)	5.8 (15%)	3.3 (16%)
Broadband	0.6 (6%)	4.8 (13%)	1.5 (6%)

Conclusions (Auroral Phenomenology)

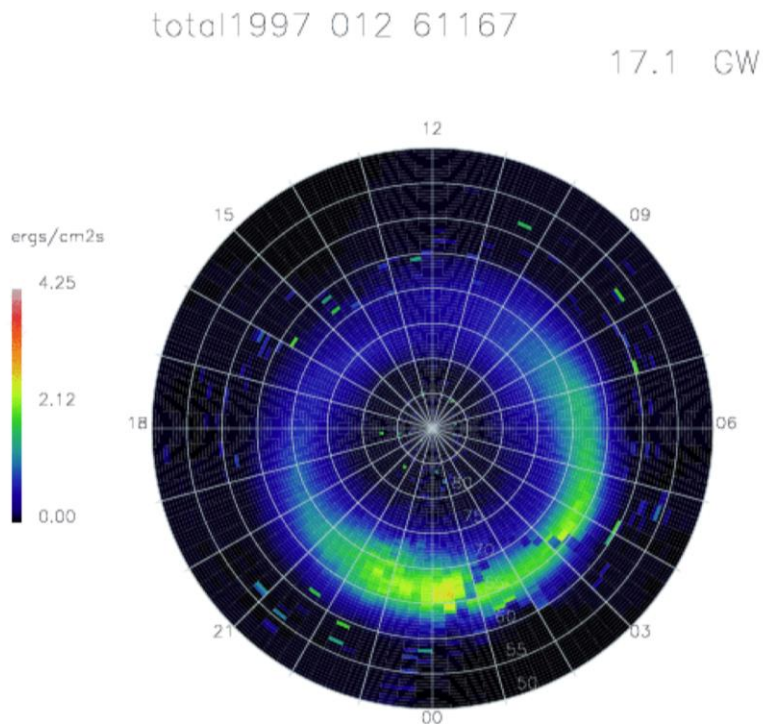
- Diffuse aurora contributes about $3/4$ of the precipitating energy flux averaged over all conditions
- Contribution from acceleration rises with higher solar wind input (but remains less than half)
- Wave aurora has the least energy flux, but rises fastest with driving. Wave aurora energy flux most resembles substorms.
- Although energy flux is mostly on the nightside, number flux is highest on the dayside.
- As solar wind driving rises, nightside dominance increases (eventually including even number flux).

Comparative Model Testing

- No existing precipitation model has undergone testing for validation.
- Imagers such as Polar UVI can estimate global auroral power on a snapshot basis, and provide a highly useful validation standard.
- Polar UVI is not sensitive to electrons below a few hundred eV, or to fluxes below about $0.25 \text{ ergs/cm}^2 \text{ s}$. Thus, even a model that perfectly predicted auroral power would not perfectly agree with UVI.



Power observed by Polar UVI:
11.3 GW



Power predicted by Ovation Prime:
12.1 GW

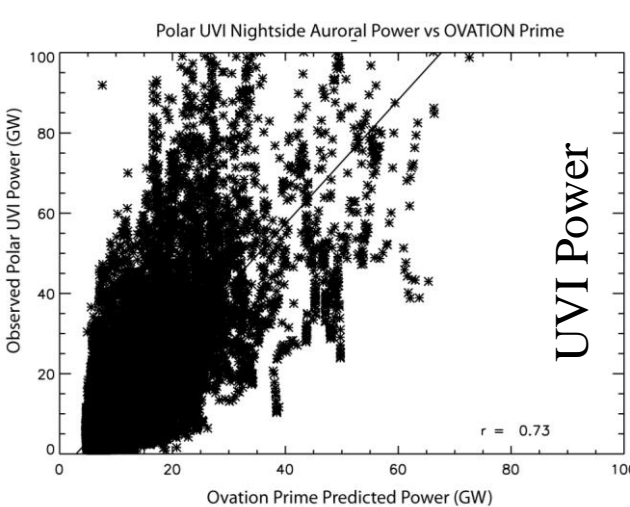
Comparison with Individual UVI Images:

> 2200 images 1996-1997

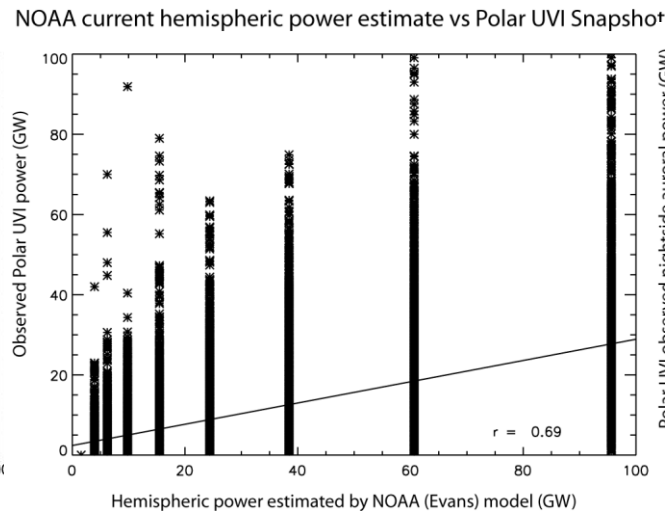
OVATION Prime solar
wind based prediction

NOAA Hemispheric
Power nowcast

Hardy Kp driven nowcast

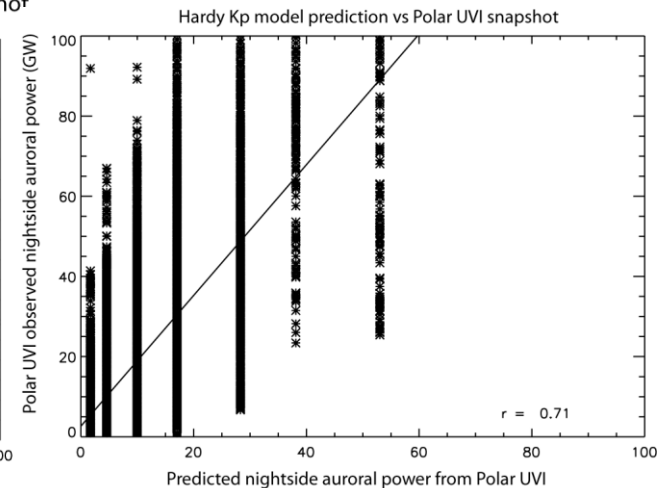


$R = 0.73$



Predicted Power

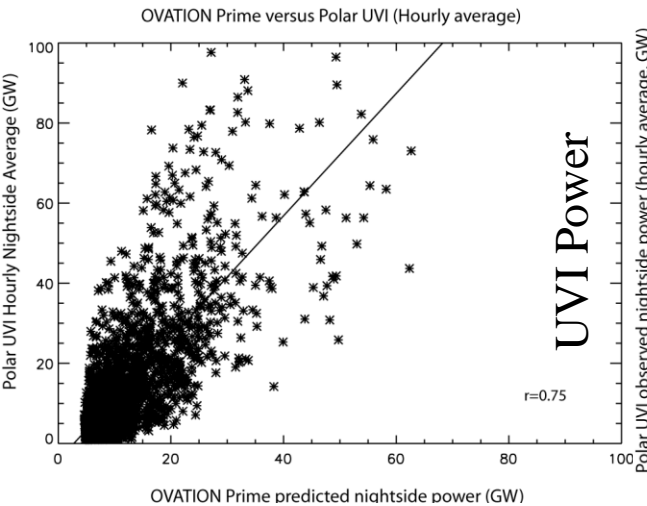
$R = 0.69$



$R = 0.71$

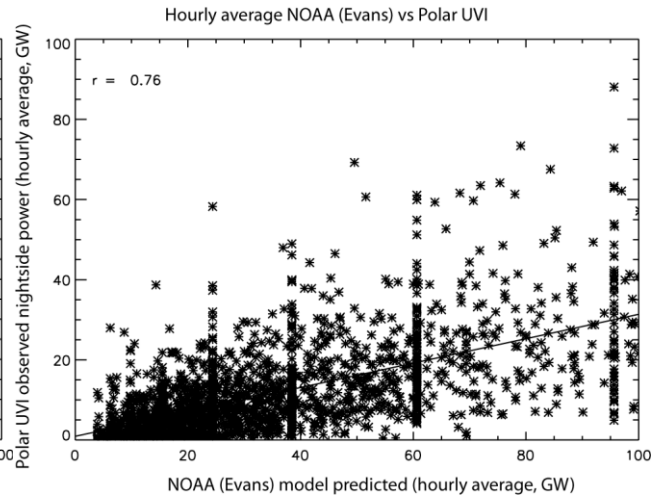
Comparison with 1-Hour Average UVI Images

OVATION Prime solar
wind based prediction



$R = 0.75$

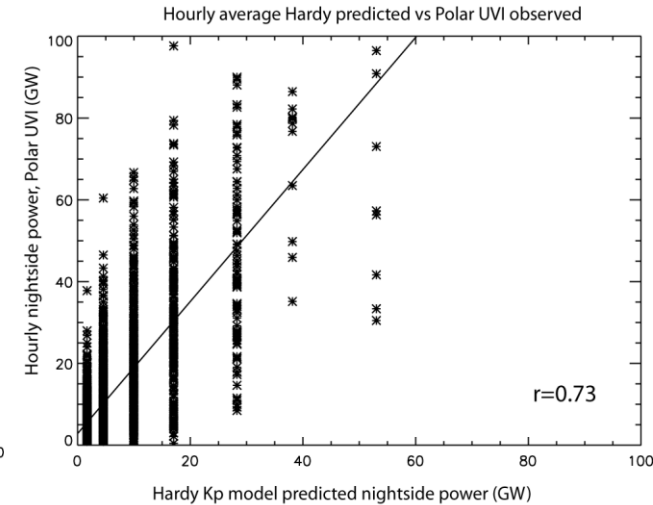
NOAA Hemispheric
Power nowcast



Predicted Power

$R = 0.76$

Hardy Kp driven nowcast



$R = 0.73$

Conclusions (Model Performance)

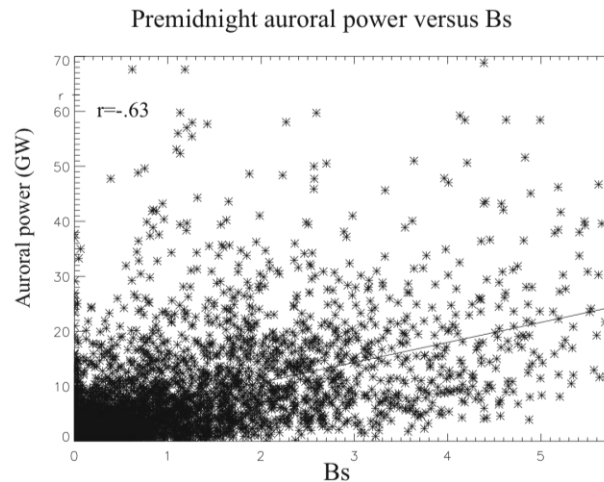
- OVATION Prime permits auroral power to be predicted based on upstream solar wind observations and performs better than these two nowcasts, instantaneously.
- NOAA Hemispheric Power index regains the lead when hour averages that include multiple passes are used.
- Nonetheless, the predictive ability of OVATION Prime is more timely than any nowcast.

Backup

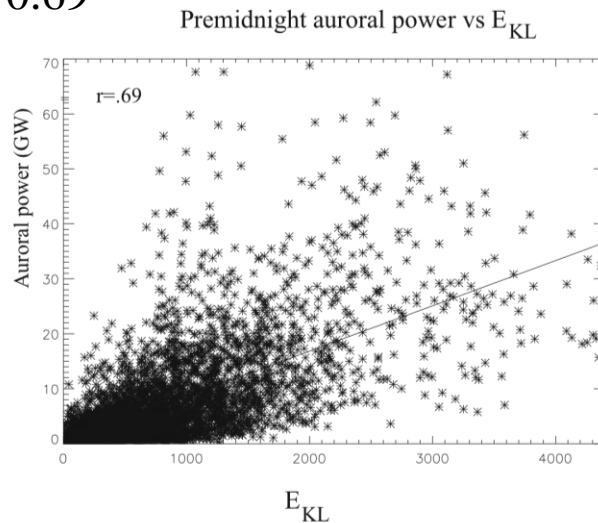
Auroral Power from Polar UVI images

Correlates Well With $d\Phi_{MP}/dt$

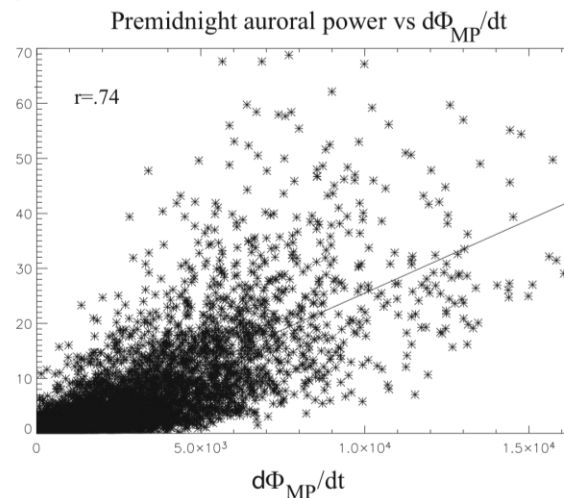
Vs. B_s : $R = 0.63$



Vs. E_{KL} : $R = 0.69$



Vs. $d\Phi_{MP}/dt$: $R = 0.74$



Seasonal Effects

- Previously, intense monoenergetic events were shown to be 3 times more frequent in winter than summer
- Total nightside auroral power is modestly higher in winter from global imagers (Polar UVI, Pixie)

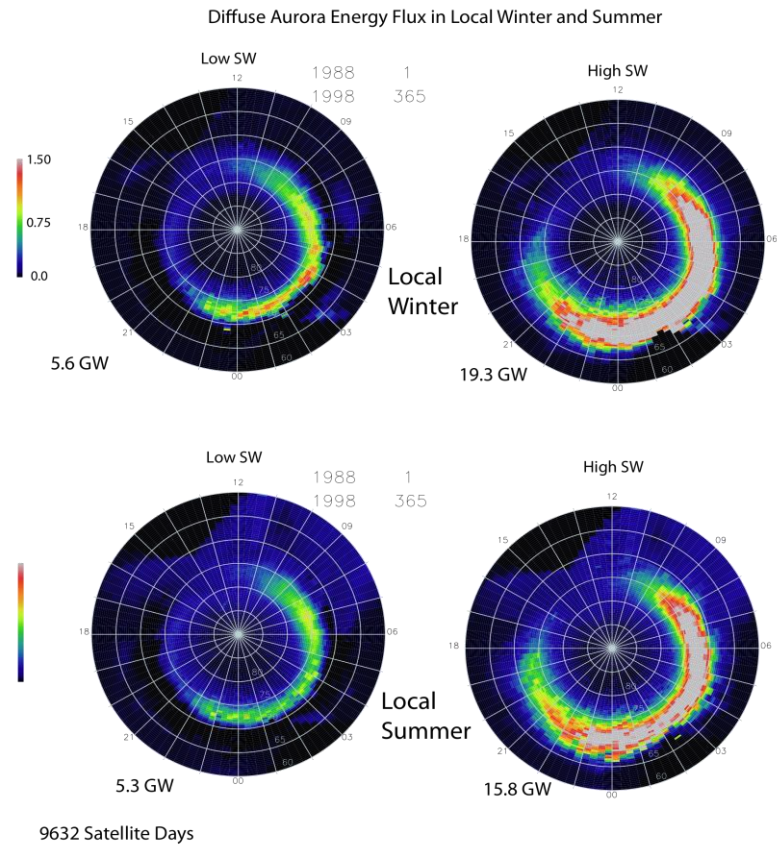


Figure 1. Diffuse aurora hemispheric energy flux for local winter (top two plots) and local summer (bottom). The left two plots are for low solar wind driving, the right two for high.

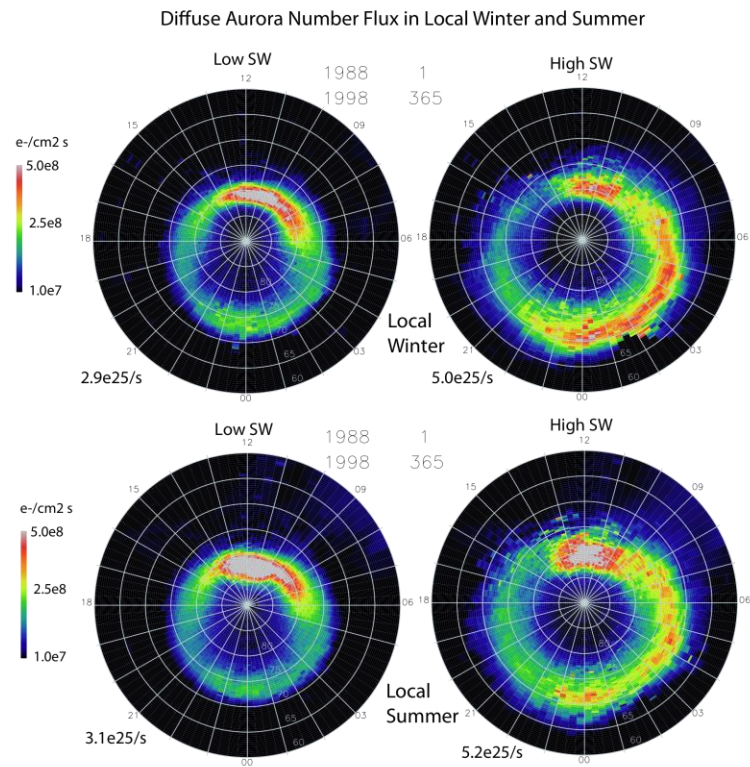
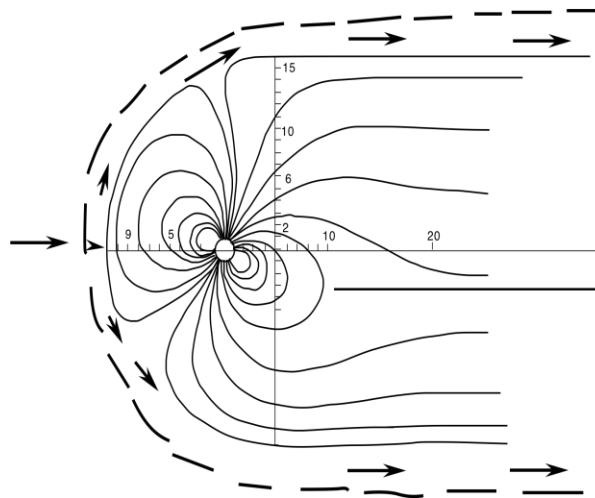


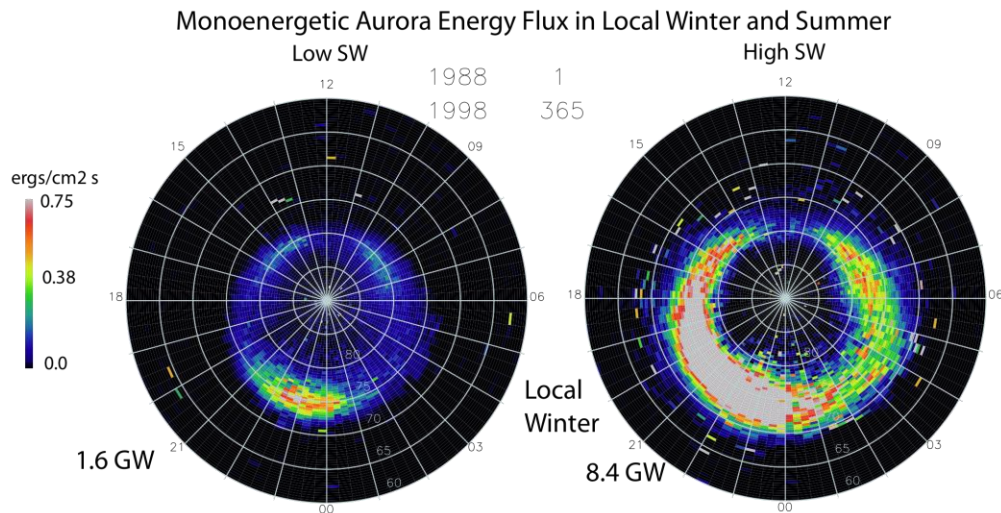
Figure 2. The diffuse aurora number flux for local winter (top two panels) and local summer (bottom two), for low solar wind driving (left two) and high solar wind driving (right two).

Magnetosheath Ions have Easier Access to Ionosphere
in the Summer Hemisphere



Ions can enter through cusp only where the bulk flow velocity
is lower than their thermal velocity

Winter



Summer

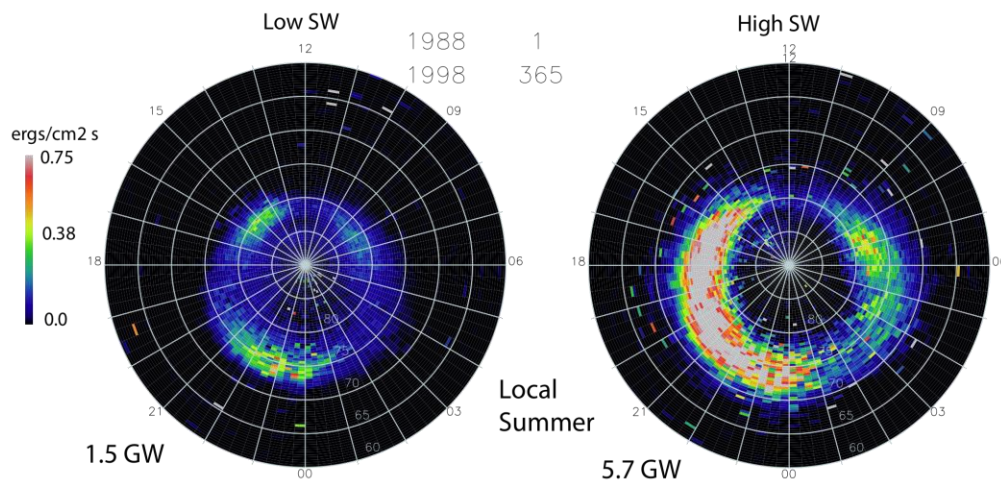
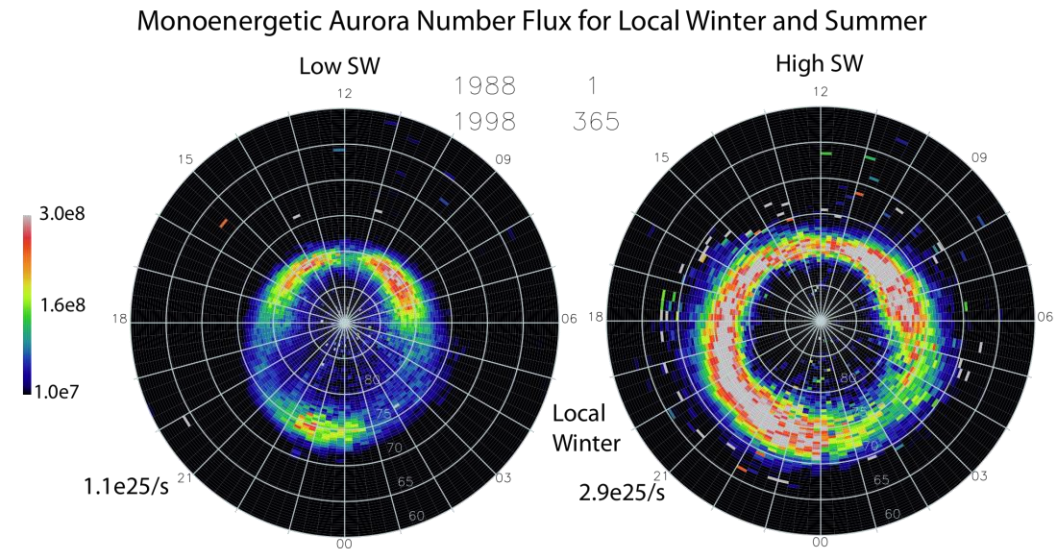


Figure 3. Monoenergetic aurora energy flux for local winter (top two panels) and summer (bottom two). Low solar wind driving is on the left, high driving on the right.

Winter



Summer

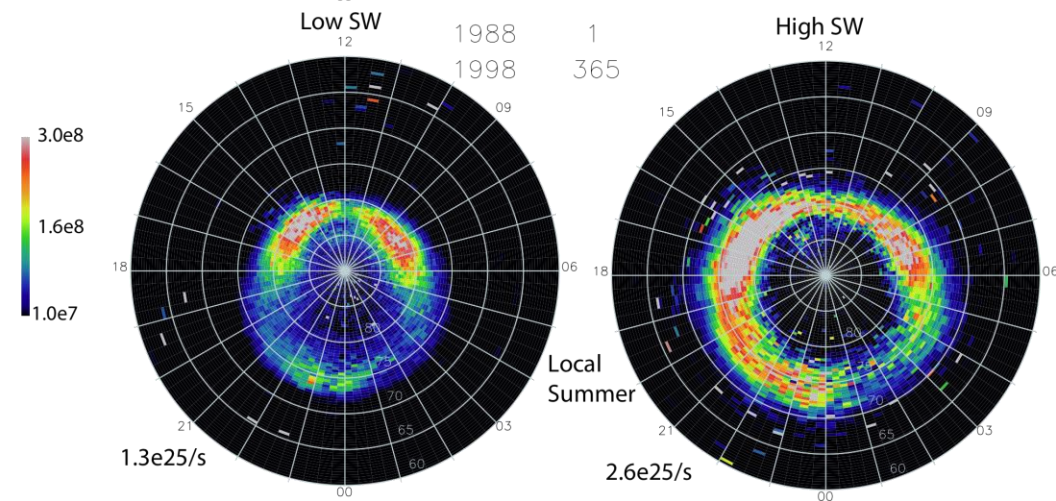
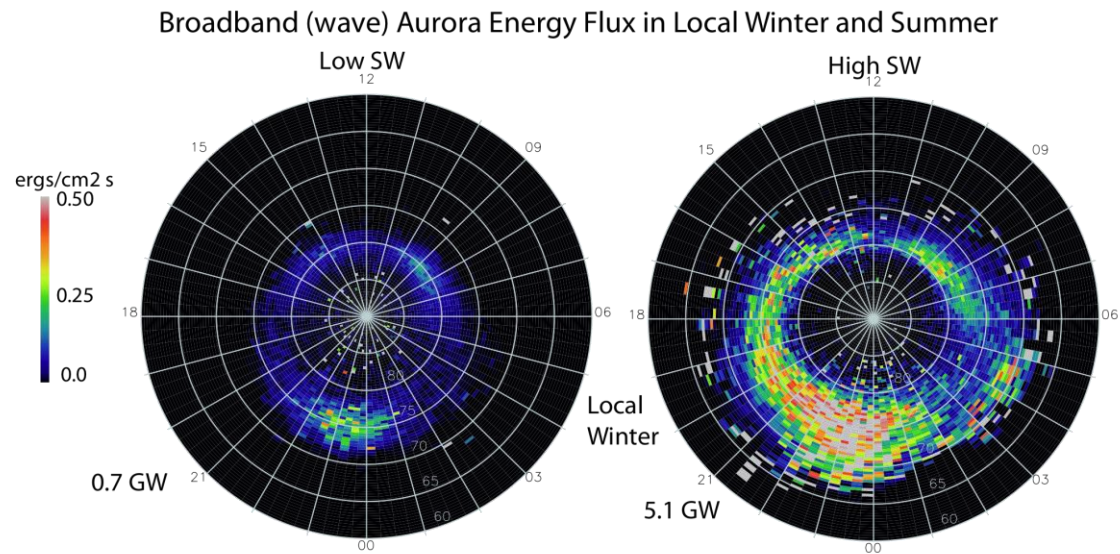
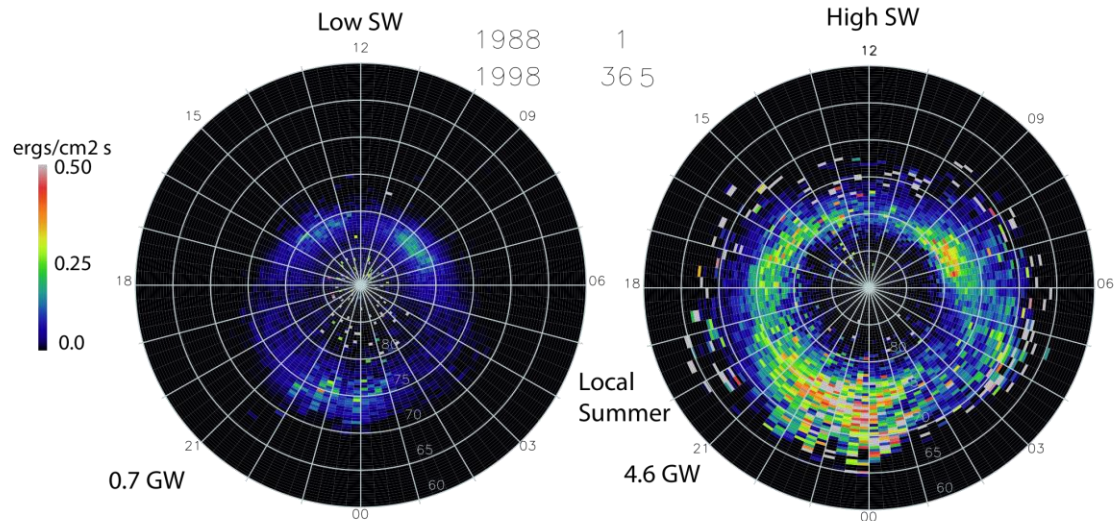


Figure 4. Monoenergetic aurora number flux for local winter (top two panels) and for summer (bottom two), under conditions of low solar wind driving (left two) and high (right two).

Winter



Summer



9632 Satellite Days

Figure 5. Broadband (wave) aurora energy flux for local winter (top two panels) and summer (bottom two). Low solar wind driving is on the left, high to the right.

Diffuse Electron Aurora Energy Flux (High solar wind driving)

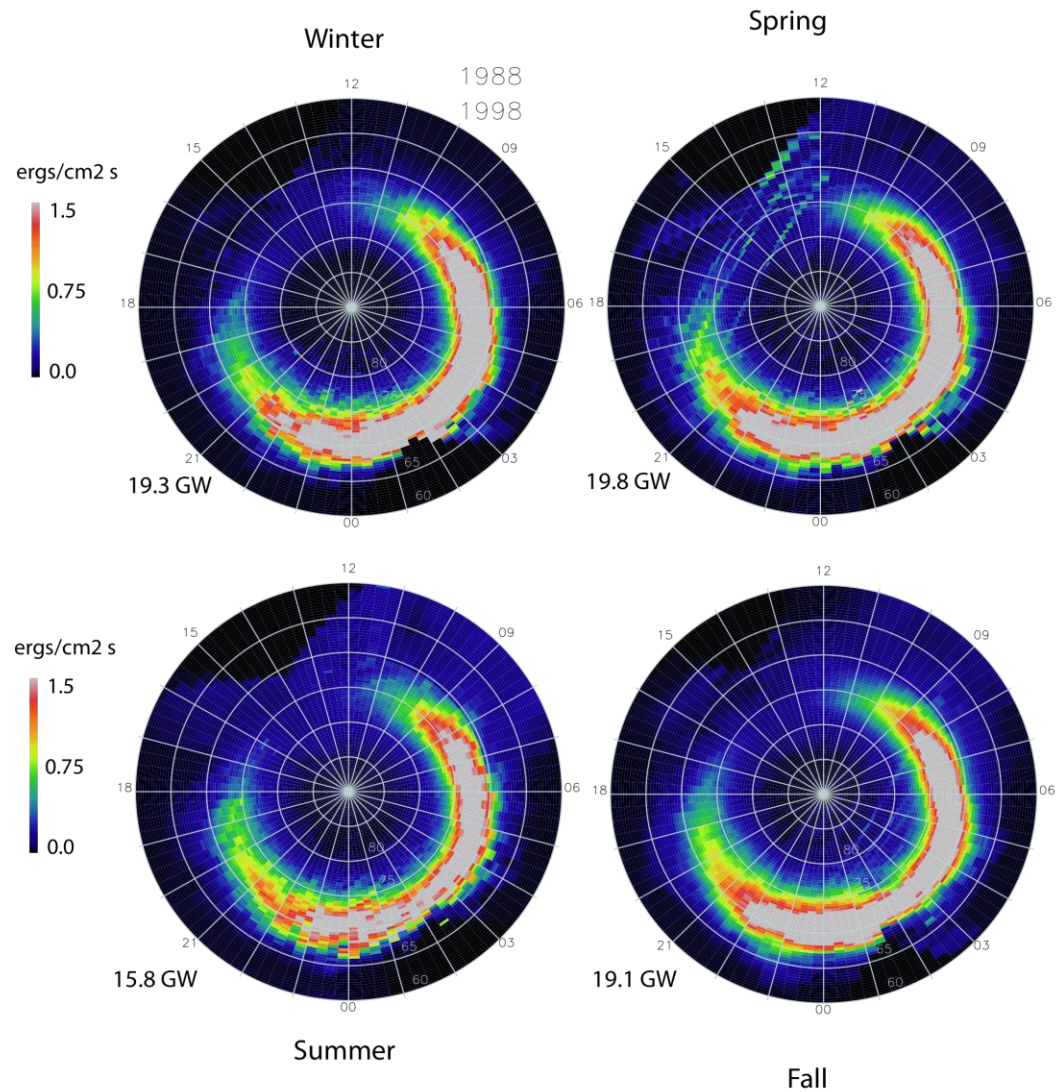


Figure 9. The diffuse electron aurora, under conditions of high solar wind driving, for all four seasons. Excepting some dayside noise during spring, the season which stands out is summer, with significantly lower nightside fluxes.

Monoenergetic Aurora Energy Flux (High Solar Wind Driving)

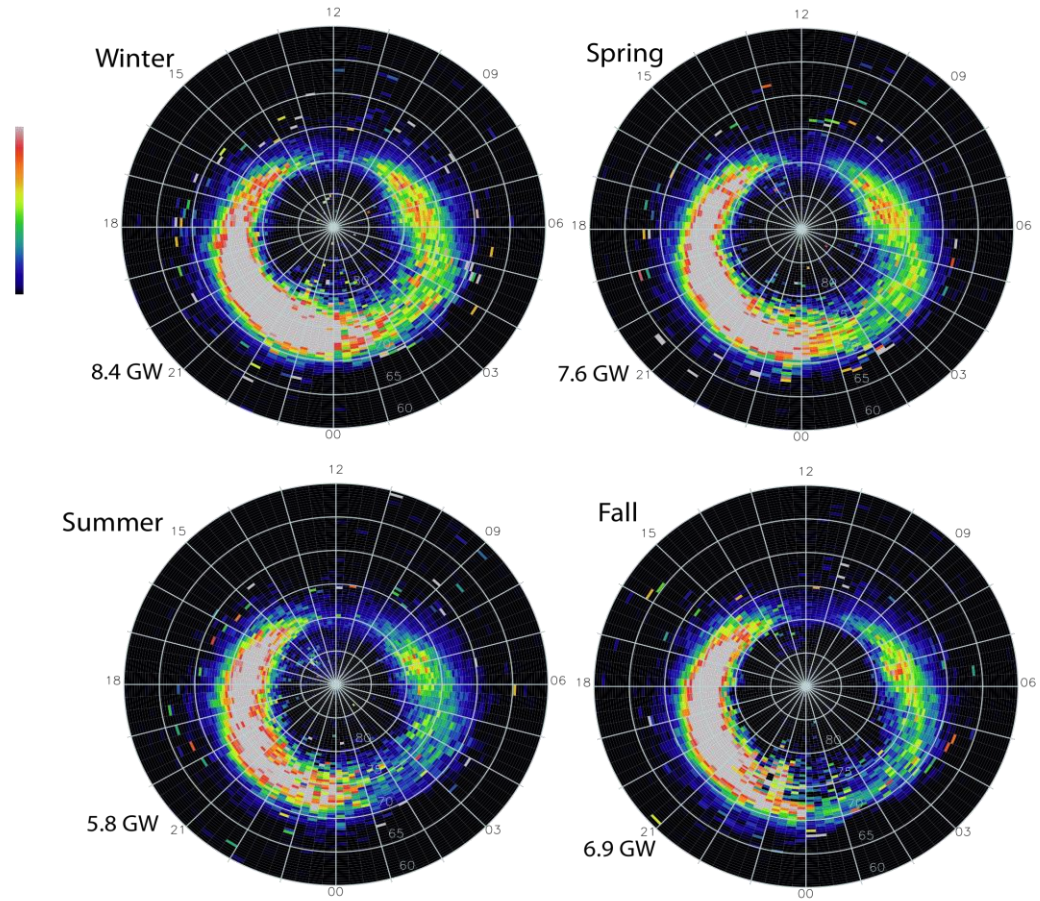


Figure 10. Monoenergetic aurora energy flux for all four seasons under conditions of high solar wind driving. Winter has the most monoenergetic aurora (on the nightside) and summer the least.

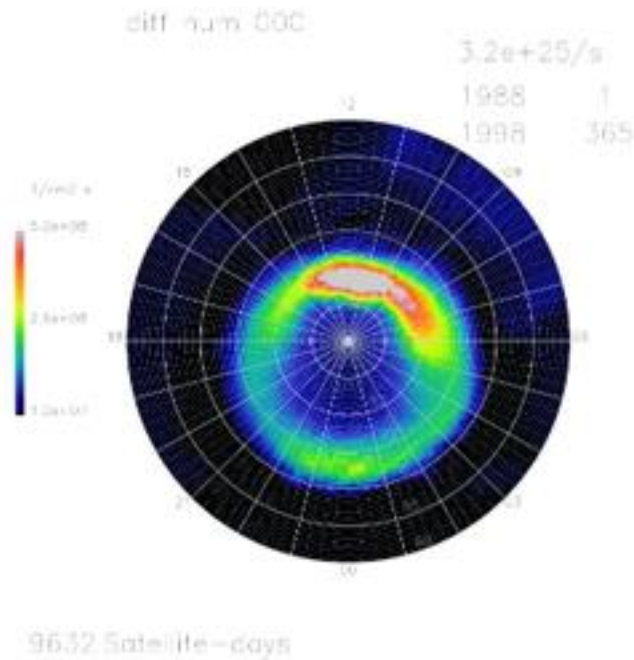
Seasonal Effects Summary

- Mono aurora has largest w/s ratio, 1.7 (night)
- Diffuse and wave are about 1.3 w/s (night)
- Ion effects are a few % (except on dayside)
- Dayside has higher energy and especially number flux in the summer (explicable)
- The nightside effects are larger in energy than number flux: implies acceleration effect

Relative Contributions to Hemispheric Precipitating Number Flux

Aurora Type	Low SW Driving	High SW Driving	All Conditions
Diffuse (e-)	3.2×10^{25} (60%)	5.4×10^{25} (48%)	4.1×10^{25} (55%)
Diffuse (ion)	2.4×10^{24} (5%)	4.1×10^{24} (4%)	3.1×10^{24} (4%)
Monoenergetic	1.1×10^{25} (21%)	2.3×10^{25} (21%)	1.6×10^{25} (21%)
Broadband	7.6×10^{24} (14%)	3.1×10^{25} (28%)	1.5×10^{25} (20%)

Diffuse (e-) Aurora Number Flux



Ion Aurora Number Flux

